Skoltech

Skolkovo Institute of Science and Technology

MASTER'S THESIS

Selection of Tensor Representations For Multiview Forecasting

Master's Educational Program: Data Science

Student: _____ Nadezhda Alsahanova
signature

Research Advisor: _____ Maxim Panov
signature
PhD, Assistant professor

Co-Advisor _____ Vadim Strijov
signature
Doctor of Physical and Mathematical Sciences, Professor

Moscow 2023

Skoltech

Skolkovo Institute of Science and Technology

МАГИСТЕРСКАЯ ДИССЕРТАЦИЯ

Выбор тензорных представлений для прогнозирования по мультимодальным измерениям.

Магистерская образовательная программа: Науки о данных

Студент: _____ Надежда Алсаханова
подпись

Научный руководитель: _____ Панов Максим Евгеньевич
подпись
к.ф.-м.н., старший преподаватель

Со-руководитель _____ Стрижов Вадим Викторович
подпись
д.ф.-м.н., профессор

Москва 2023

Selection of Tensor Representations For Multiview Forecasting

Nadezhda Alsahanova

Submitted to the Skolkovo Institute of Science and Technology on May 30, 2023

ABSTRACT

Brain-computer interfaces (BCI) are a rapidly developing research area that can help patients to restore their movement ability. The measured brain signals are highly correlated and redundant. Therefore, dimensionality reduction methods are used for stable and accurate prediction. To improve data compression during dimensionality reduction, hankelization for time series is used. However, this method has not been used in the forecasting problem in the area of BCI. In this work, we found optimal representations of feature and target tensors in latent space by combining hankelization and dimensionality reduction methods. We tested hankelization along the temporal, along the spatial, and along both dimensions. In addition, we used tree of the most common and modern dimensionality reduction models to check whether hankelization works for all models. The results on three BCI datasets showed that hankelization along both dimensions improves prediction quality the most and simplies the high-order partial least squares model. Additionally, hankelization along spatial dimension works the best way for MPCA in many cases. These results show that hankelization can improve forecasting quality in the BCI area.

Keywords: hankelization, signal decoding, ECoG, partial least squares, hybrid autoencoder, tensor regression

Research advisor:
Name: Maxim Panov
Degree, title: PhD, Assistant professor

Co-advisor:
Name: Vadim Strijov
Degree, title: Doctor of Physical and Mathematical Sciences, Professor

Contents

Chapter 1
Introduction

An initial data in the brain-computer interface's (BCI) task typically has attributes of high dimensionality, strong input correlation, and low signal-to-noise ratio. Dimensionality reduction methods are used to reduce redundancy of this data and so increase the speed of algorithms and their quality. It has previously been observed that tensorization, the generation of higher-order structured tensors from the lower-order data formats, helps to find low-rank approximation with a high level of compression and to reveal hidden correlations. There are many methods of tensorization that can be used in BCI. One of them is hankelization. Several attempts have been made to implement hankelization before the prediction of time series in different tasks. However, no previous study has investigated the influence of hankelization for the BCI area.

The thesis goal is to find optimal representations of feature and target tensors in latent space by combining a hankelization and dimensionality reduction methods. These tensors representations should be optimal in terms of forecasting quality of the target variables and complexity of methods.

Objectives:

- determine whether hankelization along temporal mode improves quality of forecasting;
- determine whether hankelization along spatial mode improves quality of forecasting;
- determine whether hankelization along both modes improve quality of forecasting;

Literature review. The BCI datasets usually contain simple target variable as classes of some movements. However, there are several datasets in which the target variable is a set of time series. These time series can be correlated and redundant as well as independent variable. One of the most popular datasets for forecasting task is food-tracking datasets by project Neurotycho [2], [17]. These datasets consist of epidural and subdural electrocorticography (ECoG) signals from monkeys. In addition, more and more human datasets for BCI forecasting are becoming available. For example, a human electroencephalography (EEG) dataset [6] has 7-channel electromyography signals from arms. The other dataset is a gesture dataset from the Stanford Digital library [11] that contains ECoG signals from humans and signals from fingers.

In the datasets for BCI, the brain signals have been taken from a large number (> 30) of closely spaced electrodes. It leads to redundant measurements and instability of models. Consequently, a great deal of previous research into BCI has focused on dimensionality reduction techniques [9]. One of the most commonly used dimensionality reduction methods is principal component analyses (PCA) and its modifications (Multilinear PCA [10]). PCA and its modifications capture the greatest variance in the input data. However, it also includes the variance in noise signals.

All the above mentioned datasets have not only correlated and noisy brain signals but also correlated target variables. Thus, dimensionality reduction of target variable also should be done. Usually, it is done by alignment between independent and target variables. Therefore, for BCI data, the widely used dimensionality reduction algorithm is partial least squares (PLS) and its modifications [4] - [22].

The algorithm projects the features and the targets onto the joint latent space and maximizes the covariances between projected vectors. It allows to save information about initial input and

target matrices and find their relations. The dimensionality of latent space is much less than the size of initial data description. It leads to a stable linear model built on the small number of features.

For the data in tensor format, there are several modifications of this algorithm, such as High-Order PLS [21], Multi-linear PLS [22] and Multi-way PLS [4]. Another similar approach to PLS is a canonical-correlation analysis (CCA). It maximizes the correlations between projected vectors of the features and the targets.

In recent years, there has been an increasing amount of literature on deep learning (DL) methods for BCI task. The most recent DL models for BCI task are Deep Tensor Canonical Correlation Analysis (DTCCA) [19] and Hybrid Autoencoder [14]. Shallow autoencoders are essentially equivalent to PCA transformations, especially when they are trained, using weight decay regularization, but autoencoders with nonlinear encoder functions and nonlinear decoder functions can learn a more powerful nonlinear generalization of PCA. Furthermore, if a condition module is added to an autoencoder for alignment with the target data, autoencoder's reduced features are connected with target data. Collectively, these studies outline a critical role for dimensionality reduction and that DL models become more prevalent in BCI task.

Despite the redundancy of data in the BCI problem, tensorization is sometimes used, which can help to catch hidden correlations and create additional informative features. Tensorization by appending an additional dimension as degrees of polynomial fittings helped to improve classification metrics [13]. Time delay embedding [5] is used to improve classification quality for BCI task. This approach was inspired by the common spectral patterns method [8] and allowed to identify bases in which the data differ substantially between classes. Moreover, for the task of artefact removal, generation of high-order tensor data for EEG was used [23]. This tensorization was made by applying wavelet transform. But none of these tensorizations has been applied in the task of predicting target time series.

One of the common tensorization techniques for time series is a hankelization. It is a natural data augmentation technique for time series to incorporate the intrinsic temporal correlation. For example, hankelization was used for anomaly detection in traffic data [18]. It has been shown that with the hankelization operation, the model can simultaneously capture the global and local spatio-temporal correlations and exhibit more robust performance. In addition, hankelization was used for forecasting for different time series data. For instance, forecasting of short term wind speed data was conducted via selective hankelization [7].

To apply hankelization for tensor data, multi-way delay embedding transform (MDT) was introduced [20]. It helped to capture some shift-invariant structure in the task of recovery of missing data. Moreover, MDT has been used to forecast short time series [16] and to forecast power consumption [15]. In both works, its ability to capture hidden correlations increased the quality of forecasting.

In this work, the influence of hankelization on the quality of prediction was studied. We considered hankelization with such dimensionality reduction models as MPCA [10], HOPLS [21] and state-of-the-art deep learning model (autoencoder) [14]. The prediction was made for four samples of data: two from the Neurotycho dataset [2], one from the gesture dataset [11] and one from the human EEG dataset [6]. The results showed...

Chapter 2
Problem statement

In this chapter, the main notations are given and the task of decoding the time series is described. An overview of standard methods of time series analysis is provided. The task of constructing an optimal linear regression model of decoding is set.

2.1 Notation

Tensors are multi-dimensional generalizations of matrices. The tensor is denoted by bold underlined capital letters, e.g., $\underline{\mathbf{X}} \in \mathbb{R}^{I_1 \times I_2 \times \ldots \times I_N}$. Matrices are denoted by boldface capital letters, e.g., $\mathbf{X} \in \mathbb{R}^{I_1 \times I_2}$, and vectors are denodet by boldface lower case letters, e.g., $\mathbf{x} \in \mathbb{R}^{I_1}$.

The element of tensor $\underline{\mathbf{X}}$ at position $(i_1, \ldots, i_N)$ will be denoted as $x_{i_1,\ldots,i_N} = \underline{\mathbf{X}}(i_1, \ldots, i_N) \in \mathbb{R}$. The order of a tensor is the number of dimensions, also known as "modes", "ways" or "dimensions".

One can define the inner product of two tensors $\underline{\mathbf{X}}$ and $\underline{\mathbf{Y}}$ as follows:

$$\langle \underline{\mathbf{X}}, \underline{\mathbf{Y}} \rangle = \sum_{i_1,i_2,\ldots,i_N} \underline{\mathbf{X}}(i_1, i_2, \ldots, i_N)\underline{\mathbf{Y}}(i_1, i_2, \ldots, i_N) = \sum_{i_1,i_2,\ldots,i_N} x_{i_1,\, i_2,\ldots,i_N} y_{i_1,\, i_2,\ldots,i_N}.$$

The norm of the tensor is defined by the inner product

$$\|\underline{\mathbf{X}}\| = \langle \underline{\mathbf{X}}, \underline{\mathbf{X}} \rangle^{1/2} = \sqrt{\sum_{i_1,i_2,\ldots,i_N} x^2_{i_1,\, i_2,\ldots,i_N}}.$$

Matricization. The mode-n matricization of the tensor $\underline{\mathbf{X}} \in \mathbb{R}^{I_1 \times I_2 \times \ldots \times I_N}$ is defined as the matrix

$$\mathbf{X}_{(n)} \in \mathbb{R}^{I_n \times I_1 \cdot I_2 \cdot \ldots \cdot I_{n-1} \cdot I_{n+1} \cdot \ldots \cdot I_N},$$

with I_n rows and $I_1 \cdot I_2 \cdot \ldots \cdot I_{n-1} \cdot I_{n+1} \cdot \ldots \cdot I_N$ columns. It is also possible to vectorize a tensor $\underline{\mathbf{X}}$. The vectorized version is

$$\text{vec}(\underline{\mathbf{X}}) \in \mathbb{R}^{I_1 \cdot I_2 \cdot \ldots \cdot I_N}.$$

Tensor Multiplication. The mode-n (multilinear) product of a tensor $\underline{\mathbf{X}} \in \mathbb{R}^{I_1 \times I_2 \times \ldots \times I_N}$ with a matrix $\mathbf{U} \in \mathbb{R}^{J \times I_n}$ is denoted by

$$\underline{\mathbf{Y}} = \underline{\mathbf{X}} \times_n \mathbf{U} \in \mathbb{R}^{I_1 \times \ldots \times I_{n-1} \times J \times I_{n+1} \times \ldots \times I_N}.$$

Elementwise, we have

$$c_{i_1 \ \ldots \ i_{n-1} \ j \ i_{n+1} \ldots \ i_N} = \sum_{i_n} x_{i_1,i_2,\, \ldots,\, i_N} u_{j i_n}.$$

The equivalent matrix form is $\mathbf{C}_{(n)} = \mathbf{B}\mathbf{A}_{(n)}$. The mode-$n$ product of a tensor $\underline{\mathbf{X}}$ with a matrix $\mathbf{U}$ is related to a change of basis in the case when a tensor defines a multilinear operator.

A full multilinear product of an Nth-order tensor, $\underline{\mathbf{X}} \in \mathbb{R}^{I_1 \times I_2 \times \ldots \times I_N}$, and a set of N factor matrices, $\mathbf{U}^{(n)} \in \mathbb{R}^{I_n \times R_n}$ for $n = 1, 2, \ldots, N$ can be compactly written as

$$\underline{\mathbf{Y}} = \underline{\mathbf{X}} \times_1 \mathbf{U}^{(1)} \times_2 \mathbf{U}^{(2)} \ldots \times_N \mathbf{U}^{(N)} = [\![\underline{\mathbf{X}};\ \mathbf{U}^{(1)}, \mathbf{U}^{(2)}, \ldots, \mathbf{U}^{(N)}]\!] \in \mathbb{R}^{R_1 \times R_2 \times \ldots \times R_N}.$$

Tucker decomposition. It provides a factorization of a Nth-order tensor into a relatively small size core tensor and factor matrices. It can be written as follows

$$\underline{\mathbf{X}} \approx [\![\underline{\mathbf{G}};\ \mathbf{U}^{(1)}, \mathbf{U}^{(2)}, \ldots, \mathbf{U}^{(N)}]\!],$$

where $\underline{\mathbf{X}} \in \mathbb{R}^{I_1 \times I_2 \times \ldots \times I_N}$ is the given tensor, $\underline{\mathbf{G}} \in \mathbb{R}^{R_1 \times R_2 \times \ldots \times R_N}$ is the core tensor $(R_n < I_n,\ n = 1, \ldots, N)$ and $\mathbf{U}^{(n)} \in \mathbb{R}^{I_n \times R_n},\ n = 1, \ldots, N$ are the factor matrices. In the standart Tucker model, factor matrices are orthogonal.

2.2 Problem statement

Definition 2.1 *A time series is a function of a discrete argument* $\mathbf{s}(t)$ *that matches time reports* $t_i \in \mathcal{T}$ *with a vector of the values of the measured variables* $\mathbf{s}(t_i) = s_i \in \mathbb{R}^M$.

Definition 2.2 *Let* $\{\mathbf{s}_n(t)\}_{n=1}^{N_s}$ *be a set of time series and* $\{\mathbf{y}_n(t)\}_{n=1}^{N_y}$ *a set of target time series. The task of finding the values of* $\{\mathbf{y}_n(t)\}_{n=1}^{N_y}$ *from the previous values of* $\{\mathbf{s}_n(t)\}_{n=1}^{N_s}$ *is called the task of decoding time series* $\{\mathbf{y}_n(t)\}_{n=1}^{N_y}$.

A dataset made from the time series $\mathbf{s}(t),\ \mathbf{y}(t)$: $(\underline{\mathbf{X}}, \underline{\mathbf{Y}})$,

$$\underline{\mathbf{X}} \in \mathbb{R}^{M \times I_1 \times \cdots \times I_{D_x}}, \qquad \underline{\mathbf{Y}} \in \mathbb{R}^{M \times J_1 \times \cdots \times J_{D_y}}, \tag{2.1}$$

where $\mathbf{y}_m = \mathbf{y}(t_m)$, $\underline{\mathbf{X}}_m \in \mathbb{R}^{I_1 \times \cdots \times I_{D_x}}$ is a tensor.

The goal is to forecast a dependent variable $\mathbf{y}_m$ from an independent input object $\underline{\mathbf{X}}_m$, $m = 1, \ldots, M$.

In this research, the aim is to find a composition of models such as:

$$\Phi = \Psi_x \circ h_x \circ g \circ h_y^{-1} \circ \Psi_y^{-1} : \quad \mathbb{R}^{I_1 \times \cdots \times I_{D_x}} \to \mathbb{R}^{J_1 \times \cdots \times J_{D_y}}, \tag{2.2}$$

where Ψ_x, h_x, g, h_y and Ψ_x work within a process:

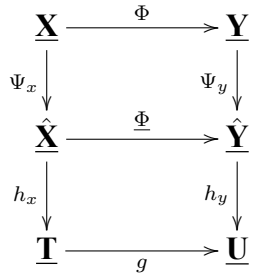

Definition 2.3 *Tensorization model* $\Psi : \mathbb{R}^{M \times I_1 \times \cdots \times I_D} \to \mathbb{R}^{\tilde{M} \times \tilde{I}_1 \times \cdots \times \tilde{I}_G}$*, where* $D < G$*, is a model that increase order of tensor from* D *to* G.

In this research, hankelization (Sec. 3.1) is used as the tensorization model. In case without tensorization, Ψ is the identity transformation. There are four types of the tensorization model used:

- Without tensorization;
- Hankelization along time dimension;
- Hankelization along space dimension;
- Hankelization along time and space dimensions.

The type of tensorization ζ is a hyperparameter of the model $\Phi(\zeta)$.

Definition 2.4 *$h : \mathbb{R}^{\tilde{I}_1 \times \cdots \times \tilde{I}_G} \to \mathbb{R}^{L_1 \times \ldots \times L_G}$, where $L_i < I_i$ is called a dimensionality reduction model, which reduces the dimensionality from $\mathbb{R}^{\tilde{I}_1 \times \cdots \times \tilde{I}_G}$ to $\mathbb{R}^{L_1 \times \ldots \times L_G}$, namely $\underline{\mathbf{T}}_m = h_x\big(\underline{\mathbf{X}}_m, \theta_y\big)$ where θ are parameters of the model.*

Definition 2.5 *$g : \mathbb{R}^{L_1 \times \ldots \times L_{G_x}} \to \mathbb{R}^{K_1 \times \ldots \times K_{G_y}}$ is called an alignment model, which aligns each $\underline{\mathbf{T}}_m \in \mathbb{R}^{L_1 \times \ldots \times L_{G_x}}$ to $\underline{\mathbf{U}}_m \in \mathbb{R}^{K_1 \times \ldots \times K_{G_y}}$, namely $\underline{\mathbf{U}}_m = g\big(\underline{\mathbf{T}}_m, \eta\big)$, where η are parameters of the model.*

Model Φ is called optimal, if it minimizes error functional $\mathcal{L}$:

$$\Phi^* = \underset{\{\theta,\eta,\zeta\}}{\arg\min}\, \mathcal{L}\left(\Phi(\underline{\mathbf{X}}, \theta, \eta, \zeta),\ \underline{\mathbf{Y}}\right). \tag{2.3}$$

In this work, we investigate how tensorization type, in combination with different dimensionality models, influences on the quality of the prediction.

Method for tensorization, hankelization, is described in the Section 3.1. Possible models of dimensionality reduction are discussed in the Sections 3.2-3.5. Tensor regression that can be used as an alignment model is described in the Section 3.7.

Chapter 3
Methodology

There are a number of instruments available for dimensionality reduction, such as principal component analysis (PCA), partial least squares (PLS), their tensor versions (High-Order PLS, MPCA) and autoencoder. These methods were used directly for the initial data or for data tensorized by its structure. In this research, hankelization was used as a tensorization method before dimensionality reduction techniques. Hankelization is one of the most common tensorization methods for time series. The benefit of this approach is that it reveals hidden correlations in initial data and allows to find low-rank approximations with high levels of compression. In this chapter, hankelization method, dimensionality reduction, and alignment models are described.

3.1 Hankelization

To begin, we will provide a standard definition of a hankelization for a vector that can be understood as a time-series signal. Let consider $\mathbf{x} = (x_1, \dots, x_I)^\top \in \mathbb{R}^I$, a hankelization of $\mathbf{x}$ with a parameter τ is given by

$$\mathcal{H}_\tau(\mathbf{x}) = \begin{pmatrix} x_1 & x_2 & \dots & x_{I-\tau+1} \\ x_2 & x_3 & \dots & x_{I-\tau+2} \\ \vdots & \vdots & \ddots & \vdots \\ x_\tau & x_{\tau+1} & \dots & x_I \end{pmatrix} \in \mathbb{R}^{\tau \times (I-\tau+1)},$$

where $\mathcal{H}_\tau(\mathbf{x})$ is a Hankel matrix of a vector $\mathbf{x}$.

Let consider a 1D convolution for vector $x \in \mathbb{R}^I$ and kernel $h \in \mathbb{R}^k$, then 1D convolution is represented by

$$x * h = \begin{pmatrix} x_1 & x_2 & \dots & x_k \\ x_2 & x_3 & \dots & x_{k+1} \\ \vdots & \vdots & \ddots & \vdots \\ x_{I-k+1} & x_{I-k+2} & \dots & x_I \end{pmatrix} \begin{pmatrix} h_1 \\ h_2 \\ \vdots \\ h_k \end{pmatrix} = \mathcal{H}_{I-k+1}(x)h.$$

Time-series have variables that are temporally nearby are highly correlated. In the BCI task, signals from different channels are also correlated. So, the data in BCI are spatially and temporally correlated. Local correlations are the reasons for the well-known advantages of extracting and combining local features before making a prediction. Convolution extracts local features by restricting the receptive fields of hidden units to be local [1]. The above mentioned connection of hankelization with convolution makes hankelization the helpful tool for revealing the hidden correlations.

Hankelization is an effective way to transform lower-order data to higher-order tensors. MDT is a multi-way extension of hankelization [20]. It combines multi-linear duplication and multi-way folding operations. By denoting $\hat{\underline{\mathbf{X}}} \in \mathbb{R}^{\tilde{I}_1 \times \dots \times \tilde{I}_G}$ as the block Hankel tensor of $\underline{\mathbf{X}} \in \mathbb{R}^{I_1 \times \dots \times I_D}$, $D < G$, the MDT for $\underline{\mathbf{X}}$ is defined by

$$\hat{\underline{\mathbf{X}}} = \mathcal{H}_\tau(\underline{\mathbf{X}}) = \text{Fold}_{(\mathbf{I},\, \tau)} \left(\underline{\mathbf{X}} \times_1 \mathbf{S}_1 \dots \times_D \mathbf{S}_D \right),$$

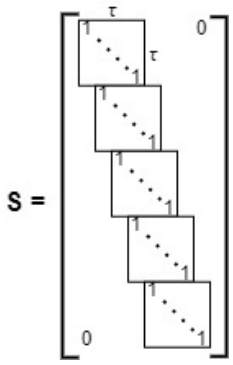

Figure 3.1: The structure of a duplication matrix **S**.

where $\mathbf{S}_d \in \mathbb{R}^{\tau_d(I_d-\tau_d+1)\times I_d}, d = 1, \ldots, D$ is a duplication matrix (see Fig. 3.1) and

$$\text{Fold}_{(I,\,\tau)} : \mathbb{R}^{\tau_1(I_1-\tau_1+1)\times \ldots \times \tau_D(I_D-\tau_D+1)} \rightarrow \mathbb{R}^{\tau_1\times(I_1-\tau_1+1)\times \ldots \times \tau_D\times(I_D-\tau_D+1)}$$

constructs a higher order block Hankel tensor $\hat{\underline{\mathbf{X}}}$ from the input tensor $\underline{\mathbf{X}}$. The inverse MDT for $\hat{\underline{\mathbf{X}}}$ is given by

$$\underline{\mathbf{X}} = \mathcal{H}_\tau^{-1}(\hat{\underline{\mathbf{X}}}) = \text{Unfold}_{(\mathbf{I},\,\tau)}(\hat{\underline{\mathbf{X}}}) \times_1 \mathbf{S}_1^\dagger \ldots \times_N \mathbf{S}_N^\dagger,$$

where † is the Moore-Penrose pseudo-inverse.

3.2 MPCA

Multilinear Principal Component Analysis (MPCA) performs feature extraction by determining a multilinear projection that captures most of the original tensorial input variation. MPCA objective is to define a multilinear transformation $\left\{\tilde{\mathbf{U}}^{(d)} \in \mathbb{R}^{I_d\times L_d},\ d = 1, \ldots, D\right\}$ that maps the original tensor space $\mathbb{R}^{I_1} \otimes \mathbb{R}^{I_2} \otimes \ldots \otimes \mathbb{R}^{I_D}$ into a tensor subspace $\mathbb{R}^{L_1} \otimes \mathbb{R}^{L_2} \otimes \ldots \otimes \mathbb{R}^{L_D}$ (with $L_d < I_d$, $d = 1, \ldots, D$):

$$\hat{\underline{\mathbf{X}}}_m \approx \underline{\mathbf{X}}_m \times_1 \tilde{\mathbf{U}}^{(1)\top} \times_2 \tilde{\mathbf{U}}^{(2)\top} \ldots \times_D \tilde{\mathbf{U}}^{(D)\top},\ \ m = 1, \ldots, M,$$

such that $\left\{\hat{\underline{\mathbf{X}}}_m \in \mathbb{R}^{L_1} \otimes \mathbb{R}^{L_2} \otimes \ldots \otimes \mathbb{R}^{L_D},\ m = 1, \ldots, M\right\}$ captures most of the variations observed in the original tensor objects, assuming that these variations are measured by the total tensor scatter $\Upsilon_{\underline{\mathbf{X}}}$ which can be calculated as follows:

$$\Upsilon_{\underline{\mathbf{X}}} = \sum_{m=1}^{M} \|\underline{\mathbf{X}}_m - \overline{\underline{\mathbf{X}}}\|_F^2,$$

where $\overline{\underline{\mathbf{X}}} = \frac{1}{M}\sum_{m=1}^{M} \underline{\mathbf{X}}_m$

The MPCA objective is the determination of the D projection matrices $\left\{\tilde{\mathbf{U}}^{(d)} \in \mathbb{R}^{I_d\times L_d},\ d = 1, \ldots, D\right\}$ that maximize the total tensor scatter $\Upsilon_{\underline{\mathbf{X}}}$

$$\left\{\tilde{\mathbf{U}}^{(d)} \in \mathbb{R}^{I_d\times L_d},\ d = 1, \ldots, D\right\} = \arg \max_{\tilde{\mathbf{U}}^{(1)},\ldots,\tilde{\mathbf{U}}^{(d)}} \Upsilon_{\underline{\mathbf{X}}}.$$

Here, the dimensionality L_d for each mode is assumed to be known or predetermined.

3.3 Partial Least Squares

The partial least squares (PLS) algorithm projects the design matrix $\mathbf{X}$ and the target matrix $\mathbf{Y}$ to the latent space with low dimensionality ($l < n$). The PLS algorithm finds the latent space matrices $\mathbf{T}, \mathbf{U} \in \mathbb{R}^{m \times l}$ that best describe the original matrices $\mathbf{X}$ and $\mathbf{Y}$.

The design matrix $\mathbf{X}$ and the target matrix $\mathbf{Y}$ are projected into the latent space in the following way:

$$\underset{m\times n}{\mathbf{X}} = \underset{m\times l}{\mathbf{T}} \cdot \underset{l\times n}{\mathbf{P}^{\mathsf{T}}} + \underset{m\times n}{\mathbf{F}} = \sum_{k=1}^{l} \underset{m\times 1}{\mathbf{t}_k} \cdot \underset{1\times n}{\mathbf{p}_k^{\mathsf{T}}} + \underset{m\times n}{\mathbf{F}}, \tag{3.1}$$

$$\underset{m\times r}{\mathbf{Y}} = \underset{m\times l}{\mathbf{U}} \cdot \underset{l\times r}{\mathbf{Q}^{\mathsf{T}}} + \underset{m\times r}{\mathbf{E}} = \sum_{k=1}^{l} \underset{m\times 1}{\mathbf{u}_k} \cdot \underset{1\times r}{\mathbf{q}_k^{\mathsf{T}}} + \underset{m\times r}{\mathbf{E}}, \tag{3.2}$$

where $\mathbf{T}$ and $\mathbf{U}$ are the scores matrices in the latent space, $\mathbf{P}$ and $\mathbf{Q}$ are the loading matrices, $\mathbf{E}$ and $\mathbf{F}$ are residual matrices. The PLS maximizes the linear relation between the columns of matrices $\mathbf{T}$ and $\mathbf{U}$ as

$$\mathbf{U} \approx \mathbf{TB}, \quad \mathbf{B} = \operatorname{diag}(\beta_k), \quad \beta_k = \mathbf{u}_k^{\mathsf{T}}\mathbf{t}_k / (\mathbf{t}_k^{\mathsf{T}}\mathbf{t}_k).$$

We use the PLS algorithm as the dimensionality reduction algorithm in this research.

To obtain the model prediction and find the model parameters, we multiply both sides of (3.1) by $\mathbf{W}$. Since the residual matrix $\mathbf{E}$ rows are orthogonal to the columns of $\mathbf{W}$, we have

$$\mathbf{XW} = \mathbf{TP}^{\mathsf{T}}\mathbf{W}.$$

The linear transformation between objects in the input and latent spaces is the following

$$\mathbf{T} = \mathbf{XW}^*, \quad \text{where } \mathbf{W}^* = \mathbf{W}(\mathbf{P}^{\mathsf{T}}\mathbf{W})^{-1}. \tag{3.3}$$

The matrix of the model parameters $\mathbf{\Theta}$ could be found from the equations (3.2) and (3.3) as

$$\mathbf{Y} = \mathbf{UQ}^{\mathsf{T}} + \mathbf{E} \approx \mathbf{TBQ}^{\mathsf{T}} + \mathbf{E} = \mathbf{XW}^*\mathbf{BQ}^{\mathsf{T}} + \mathbf{E} = \mathbf{X\Theta} + \mathbf{E}. \tag{3.4}$$

Thus, the model parameters (3.7) are equal to

$$\mathbf{\Theta} = \mathbf{W}(\mathbf{P}^{\mathsf{T}}\mathbf{W})^{-1}\mathbf{BQ}^{\mathsf{T}}.$$

The final model (3.4) is a linear model that is low-dimensional in the latent space. It reduces the data redundancy and increases the model stability.

3.4 High-Order PLS

HOPLS performs simultaneously constrained Tucker decompositions for an $(D+1)$th-order independent tensor, $\underline{\mathbf{X}} \in \mathbb{R}^{M \times I_1 \times \ldots \times I_D}$, and an $(D+1)$th-order dependent tensor, $\underline{\mathbf{Y}} \in \mathbb{R}^{M \times J_1 \times \ldots \times J_D}$, which have the same size in the first mode. Such a model allows us to find the optimal subspace approximation of $\underline{\mathbf{X}}$, in which the independent and dependent variables share a common set of latent vectors in one specific mode (i.e.,samples mode).

$$\underline{\mathbf{X}} = \sum_{r=1}^{R} \underline{\mathbf{G}}_{xr} \times_1 \mathbf{t}_r \times_2 \mathbf{P}_r^{(1)} \ldots \times_{D+1} \mathbf{P}_r^{(D)} + \underline{\mathbf{E}}_R,$$

$$\underline{\mathbf{Y}} = \sum_{r=1}^{R} \underline{\mathbf{G}}_{yr} \times_1 \mathbf{t}_r \times_2 \mathbf{Q}_r^{(1)} \ldots \times_{D+1} \mathbf{Q}_r^{(D)} + \underline{\mathbf{F}}_R,$$

where R is the number of latent vectors, $\mathbf{t}_r \in \mathbb{R}^M$ is the r-th latent vector, $\left\{\mathbf{P}_r^{(d)}\right\}_{d=1}^{D} \in \mathbb{R}^{I_d \times L_d}$ and $\left\{\mathbf{Q}_r^{(d)}\right\}_{d=1}^{D} \in \mathbb{R}^{J_d \times K_d}$ are the loading matrices in mode-d, and $\underline{\mathbf{G}}_{xr} \in \mathbb{R}^{1 \times L_1 \times \ldots \times L_D}$ and $\underline{\mathbf{G}}_{yr} \in \mathbb{R}^{1 \times K_1 \times \ldots \times K_D}$ are core tensors.

By defining a latent matrix $\mathbf{T} = \left[\mathbf{t}_1, \ldots, \mathbf{t}_R\right]$, mode-$d$ loading matrix $\overline{\mathbf{P}}^{(d)} = \left[\mathbf{P}_1^{(d)}, \ldots, \mathbf{P}_R^{(d)}\right]$, mode-$d$ loading matrix $\overline{\mathbf{Q}}^{(d)} = \left[\mathbf{Q}_1^{(d)}, \ldots, \mathbf{Q}_R^{(d)}\right]$ and core tensors

$$\underline{\mathbf{G}}_x = \text{blockdiag}\left(\underline{\mathbf{G}}_{x1}, \ldots, \underline{\mathbf{G}}_{xR}\right) \in \mathbb{R}^{R \times RL_1 \times \ldots \times RL_D},$$
$$\underline{\mathbf{G}}_y = \text{blockdiag}\left(\underline{\mathbf{G}}_{y1}, \ldots, \underline{\mathbf{G}}_{yR}\right) \in \mathbb{R}^{R \times RK_1 \times \ldots \times RK_D},$$

the HOPLS model can be rewritten as

$$\underline{\mathbf{X}} = \underline{\mathbf{G}}_x \times_1 \mathbf{T} \times_2 \overline{\mathbf{P}}^{(1)} \ldots \times_{D+1} \overline{\mathbf{P}}^{(D)} + \underline{\mathbf{E}}_R,$$
$$\underline{\mathbf{Y}} = \underline{\mathbf{G}}_y \times_1 \mathbf{T} \times_2 \overline{\mathbf{Q}}^{(1)} \ldots \times_{D+1} \overline{\mathbf{Q}}^{(D)} + \underline{\mathbf{F}}_R,$$

where $\underline{\mathbf{E}}_R$ and $\underline{\mathbf{F}}_R$ are the residuals obtained after extracting R latent components. The core tensors, $\underline{\mathbf{G}}_x$ and $\underline{\mathbf{G}}_y$, have a special block-diagonal structure (Fig. 3.2) and their elements indicate the level of local interactions between the corresponding latent vectors and loading matrices.

The cross-covariance tensor is defined by

$$\underline{\mathbf{C}} = COV_{\{1,1\}}(\underline{\mathbf{X}}, \underline{\mathbf{Y}}) \in \mathbb{R}^{I_1 \times \ldots \times I_D \times J_1 \times \ldots \times J_D}$$

The optimization problem can be formulated as

$$\left\| \left[\!\left[\underline{\mathbf{C}}; \mathbf{P}^{(1)\top}, \ldots, \mathbf{P}^{(D)\top}, \mathbf{Q}^{(1)\top}, \ldots, \mathbf{Q}^{(D)\top} \right]\!\right] \right\|_F^2 \rightarrow \max_{\substack{\left\{\mathbf{P}^{(d)}, \mathbf{Q}^{(d)}\right\}, \\ \text{s.t. } \mathbf{P}^{(d)\top}\mathbf{P}^{(d)} = \mathbf{I}_{L_d}, \\ \mathbf{Q}^{(d)\top}\mathbf{Q}^{(d)} = \mathbf{I}_{K_d}}},$$

where $[\![\ldots]\!]$ denotes the multilinear products between a tensor and a set of matrices, $\mathbf{P}^{(d)}$ and $\mathbf{Q}^{(d)}, d = 1, \ldots, D$, comprise the unknown parameters.

3.5 Autoencoder ReducedNet

Autoencoders are often used for the problem of dimensionality reduction. For example, for the task of reducing the dimension for electrocorticogram data, the hybrid autoencoder ReducedNet [14] was used. Predicting the coordinates of hand movements is found to be more accurate after dimensionality reduction using ReducedNet than after methods such as PLS or KernelPCA. Therefore, it was decided to apply this model in this work as state-of-art model, but with minor modifications.

The model proposed in [14] consists of two blocks: a dimensionality reduction module consisting of an encoder h and a decoder ψ; and a condition module ω. The dimensionality reduction module is composed of convolutional blocks (Conv1D) and LSTM blocks. Each convolutional block contains of a one-dimensional convolutional layer, one Batch Normalization layer, GELU (gaussian error linear unit) activation function layer and Dropout layer. An LSTM block is a single LSTM layer. The condition module was a single linear layer.

The ReducedNet model has only one tunable parameter, N_{CH}, that was the number of features after encoder.

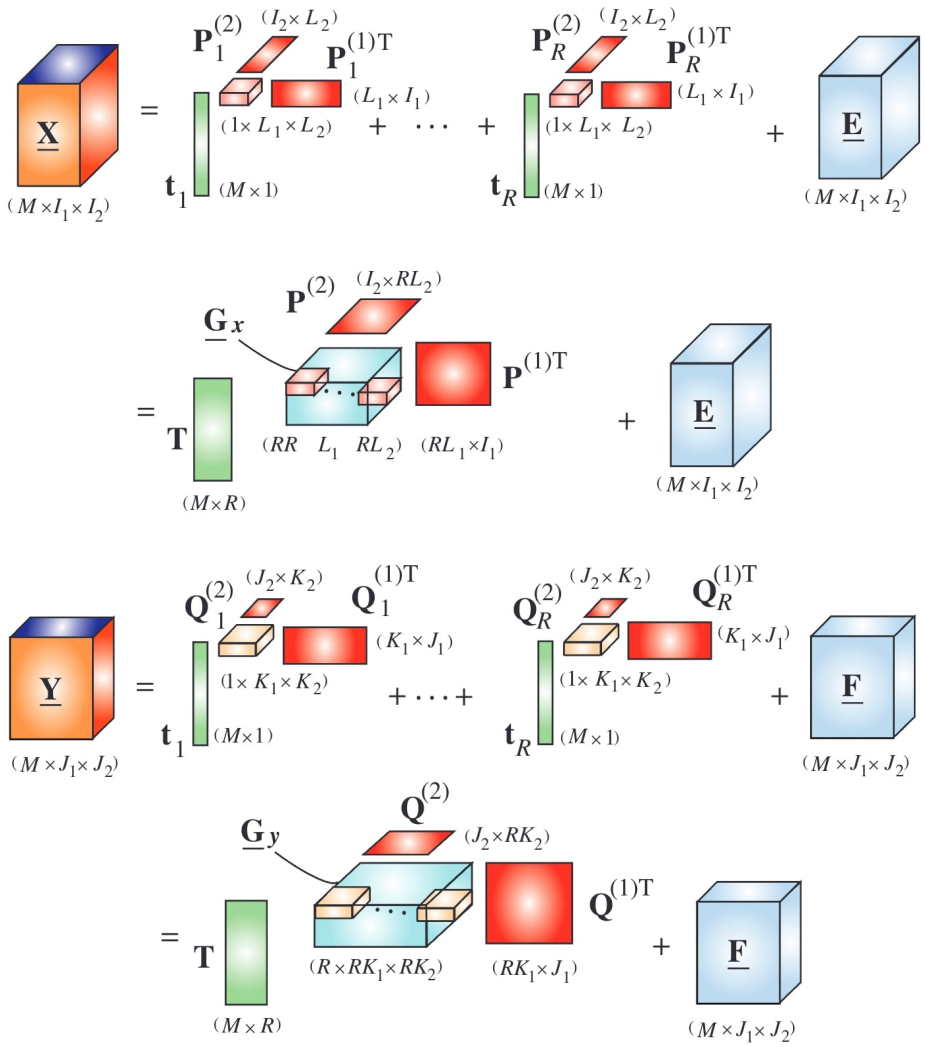

Figure 3.2: The HOPLS model which approximates the independent variables, $\underline{\mathbf{X}}$, as a sum of rank-$(1, L_1, L_2)$ tensors. The approximation for the dependent variables, $\underline{\mathbf{Y}}$, follows a similar principle, whereby the common latent components, $\mathbf{T}$, are shared between $\underline{\mathbf{X}}$ and $\underline{\mathbf{Y}}$. This picture is taken from [3].

The loss, proposed in article [14], takes into account outputs from both modules:

$$\mathcal{L}_1 = \mathcal{L}_{rec} + \alpha \cdot \mathcal{L}_{dec}, \tag{3.5}$$

where reconstruction loss is defined as follows:

$$\mathcal{L}_{rec} = \frac{1}{M} \sum_{m=1}^{M} \|\underline{\mathbf{X}}_m - h \circ \psi(\underline{\mathbf{X}}_m)\|^2,$$

and decoding loss is given by

$$\mathcal{L}_{dec} = \frac{1}{M} \sum_{m=1}^{M} \|\mathbf{Y}_m - \omega \circ h(\underline{\mathbf{X}}_m)\|^2.$$

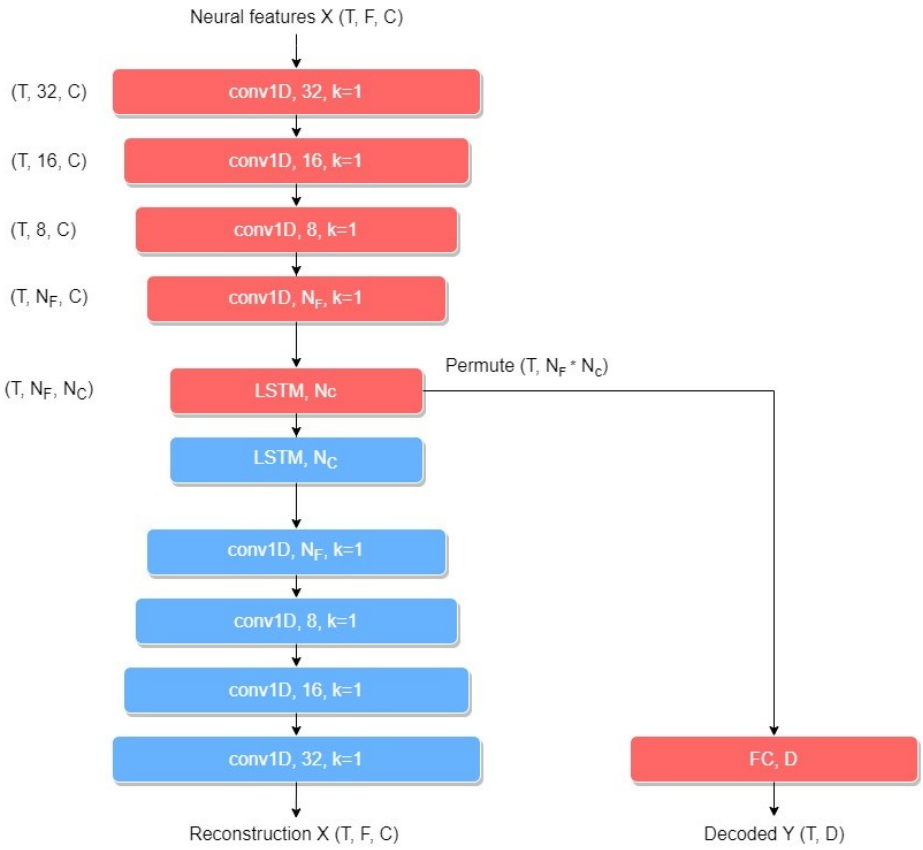

Figure 3.3: TensorReducedNet.

Modification of ReducedNet. The main problem of ReducedNet is that encoder's output is a matrix. It means that the input tensor loses its initial structure. Besides, it can work only with 3D data. Thus, in this work, TensorReducedNet is proposed. TensorReducedNet can be applyed to the data with any number of dimensions and it's encoders output is a tensor. The 3D example of TensorReducedNet can be seen in Fig. 3.3. The output from the encoder of 3D TensorReducedNet is in $\mathbb{R}^{T \times N_F \times N_{CH}}$.

For tensors with order higher than 3, the reduction of dimensionality of all modes except one is achieved by convolutional blocks, the reduction of dimensionality of the last mode (temporal) is made by LSTM. For autoencoder with output in $\mathbb{R}^{T \times L_1 \times L_2 \times \ldots \times L_G}$ the changes done by encoder are the follows:

$$\underline{\mathbf{X}} \in \mathbb{R}^{M \times I_1 \times \ldots \times I_G} \xrightarrow{\text{conv1D blocks}} \tilde{\underline{\mathbf{X}}} \in \mathbb{R}^{M \times I_1 \times L_2 \times \ldots \times L_G} \xrightarrow{\text{LSTM block}} \hat{\underline{\mathbf{X}}} \in \mathbb{R}^{M \times L_1 \times L_2 \times \ldots \times L_G}.$$

The FC layer for TensorReducedNet is applied to the unfolded tensor $\hat{\underline{\mathbf{X}}}$ along first mode.

3.6 Multimodal regression

The feature tensor $\underline{\mathbf{X}}$ has $D+1$ dimension. To restore the target time series, the feature tensor $\underline{\mathbf{X}}$ can be unfolded by the first dimension:

$$\underline{\mathbf{X}}_{(1)} = \left[\text{vec}\left(\underline{\mathbf{X}}_1\right)^\top, \ldots, \text{vec}\left(\underline{\mathbf{X}}_M\right)^\top\right]^\top \in \mathbb{R}^{M \times (I_1 \cdot \ldots \cdot I_D)} \tag{3.6}$$

Thus, the problem becomes a multimodal regression problem, where $\mathbf{X} \in \mathbb{R}^{M \times (I_1 \cdot \ldots \cdot I_D)}$ is the input matrix obtained by matricization of the input tensor, $\mathbf{Y} \in \mathbb{R}^{M \times J}$ is the target matrix.

The goal is to forecast a dependent variable $\mathbf{y}_m \in \mathbb{R}^J$ with J targets from an independent input object $\mathbf{x}_m \in \mathbb{R}^I$ with $I = I_1 \cdot \ldots \cdot I_D$ features. We assume that there is a linear dependence between the object $\mathbf{x}_m$ and the target variable $\mathbf{y}_m$ as

$$\mathbf{y}_m = \boldsymbol{\Theta}\mathbf{x}_m + \boldsymbol{\varepsilon}, \tag{3.7}$$

where $\boldsymbol{\Theta} \in \mathbb{R}^{J \times I}$ is the matrix of the model parameters, and $\boldsymbol{\varepsilon} \in \mathbb{R}^J$ is a residual vector. One has to find the matrix of the model parameters $\boldsymbol{\Theta}$ by a given dataset $(\mathbf{X}, \mathbf{Y})$, where $\mathbf{X} \in \mathbb{R}^{M \times I}$ is a design matrix and $\mathbf{Y} \in \mathbb{R}^{M \times J}$ is a target matrix:

$$\mathbf{X} = [\mathbf{x}_1, \ldots, \mathbf{x}_m]^\mathsf{T} = [\boldsymbol{\chi}_1, \ldots, \boldsymbol{\chi}_n]; \quad \mathbf{Y} = [\mathbf{y}_1, \ldots, \mathbf{y}_m]^\mathsf{T} = [\boldsymbol{\nu}_1, \ldots, \boldsymbol{\nu}_r].$$

The columns $\boldsymbol{\chi}_j$ of $\mathbf{X}$ correspond to the object features, and the columns $\boldsymbol{\nu}_j$ of $\mathbf{Y}$ correspond to the targets.

The optimal parameters are determined by the minimization of an error function. We define the quadratic loss function as follows:

$$\mathcal{L}(\boldsymbol{\Theta}|\mathbf{X}, \mathbf{Y}) = \left\| \underset{M \times J}{\mathbf{Y}} - \underset{M \times I}{\mathbf{X}} \cdot \underset{J \times I}{\boldsymbol{\Theta}}^\mathsf{T} \right\|_2^2 \to \min_{\boldsymbol{\Theta}}. \tag{3.8}$$

The solution of (3.8) is given by

$$\boldsymbol{\Theta} = \mathbf{Y}^\mathsf{T}\mathbf{X}(\mathbf{X}^\mathsf{T}\mathbf{X})^{-1}.$$

The linear dependent columns of $\mathbf{X}$ lead to an instable solution for the optimization problem (3.8). If there is a vector $\boldsymbol{\alpha} \neq \mathbf{0}_I$ such that $\mathbf{X}\boldsymbol{\alpha} = \mathbf{0}_m$, then adding $\boldsymbol{\alpha}$ to any column of $\boldsymbol{\Theta}$ does not change the value of the loss function $\mathcal{L}(\boldsymbol{\Theta}|\mathbf{X}, \mathbf{Y})$. In this case, the matrix $\mathbf{X}^\mathsf{T}\mathbf{X}$ is close to singular and is not invertible. One of the possible solutions is not to make a matricization of the input tensor but to use tensor regression. The main advantage of the tensor regression over the multimodal regression is that it stores information about the data structure.

3.7 Tensor regression

The tensor regression can be defined in a similar way as (3.7):

$$\mathbf{y}_m = \langle \underline{\mathbf{X}}_m | \underline{\mathbf{W}} \rangle + \varepsilon, \tag{3.9}$$

where $\langle \underline{\mathbf{X}}_m | \underline{\mathbf{W}} \rangle$ is a tensor contraction along the first D dimensions of the D-dimensional initial tensor $\underline{\mathbf{X}}_m \in \mathbb{R}^{I_1 \times \cdots \times I_D}$ and $(D+1)$-dimensional tensor of model parameters $\underline{\mathbf{W}} \in \mathbb{R}^{I_1 \times \cdots \times I_D \times J}$, $\varepsilon \in \mathbb{R}^J$ is an error, $\mathbf{y}_m \in \mathbb{R}^J$ is the target vector.

The j-th element of the vector obtained after tensor contraction of $\underline{\mathbf{X}}_m$ and $\underline{\mathbf{W}}$ is calculated as follows:

$$\langle \underline{\mathbf{X}}_m | \underline{\mathbf{W}} \rangle_j = \sum_{i_1=1}^{I_1} \cdots \sum_{i_D=1}^{I_D} x_{i_1,\ldots,i_D} w_{i_1,\ldots,i_D,k} \tag{3.10}$$

The optimal parameter tensor $\underline{\mathbf{W}}^*$ is found by minimizing the quadratic error function:

$$\underline{\mathbf{W}}^* = \arg\min_{\underline{\mathbf{W}}} \sum_{m=1}^{M} \left\| \mathbf{y}_m - \langle \underline{\mathbf{X}}_m | \underline{\mathbf{W}} \rangle \right\|_2^2 \tag{3.11}$$

In practice, the parameter tensor $\underline{\mathbf{W}}$ is represented in the Tucker decomposition:

$$\underline{\mathbf{W}} \approx \underline{\mathbf{G}} \times_1 \mathbf{U}^{(1)} \ldots \times_D \mathbf{U}^{(D)} \times_{D+1} \mathbf{U}^{(D+1)}, \tag{3.12}$$

where $\underline{\mathbf{G}}$ is a smaller core tensor, $\mathbf{U}^{(i)}$ are unitary matrices.

For higher-order $\underline{\mathbf{Y}} \in \mathbb{R}^{M \times J_1 \times \ldots \times J_D}$, unfolded tensor $\underline{\mathbf{Y}}$ along the first mode is used as $\mathbf{Y} \in \mathbb{R}^{M \times J}$ where $J = J_1 \cdot \ldots \cdot J_D$.

Chapter 4
Numerical experiments

The proposed method of applying hankelization before dimensionality reduction was tested on real data. The goal of the experiment was to investigate whether hankelization helps to improve quality of three different dimensionality reduction models for multiview BCI datasets. These models are MPCA, HOPLS and Hybrid Autoencoder (TensorReducedNet). In this chapter, datasets used in this work are described, metrics for performance evaluation are defined, and results are performed and discussed.

4.1 Datasets

In this section the datasets used in this work will be described. All datasets are multiview, as they have many channels. The datasets are differs in number of channels and method of receiving brain signals (EEG, ECoG).

4.1.1 Neurotycho dataset

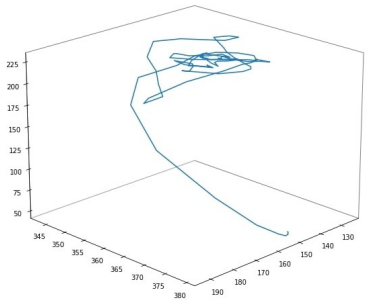

Figure 4.1: Hand movement trajectory

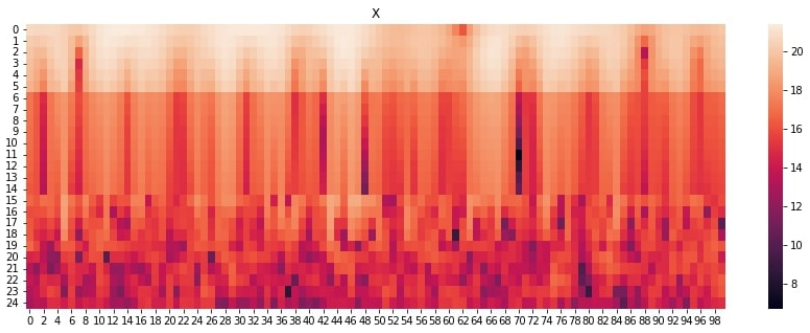

Figure 4.2: One channel data in time-frequency domain

One of the datasets for the computational experiment is electrocorticogram (ECoG) data from the Neurotycho [17] dataset. The data consist of 32-channel voltage signals taken from the monkey's brain. ECoG data are multidimensional and measurements correlate in both temporal and spatial domains. The target variable is the coordinates of the position of the hand in space (Fig. 4.1).

The original voltage signals were converted into a time-frequency representation using a wavelet transform with a parent Morlet wavelet, since this type of transformation is often used in problems with ECoG data [4], [2]. Frequencies was chosen as in [12]. The description of the source signal at each time had the dimension 32 (channels) $\times 27$ (frequencies) $= 864$. Each signal represented a local time interval with a duration of $\Delta t = 1s$. The time step between the signals $\delta t = 0.05s$. The data had dimensions $\underline{\mathbf{X}} \in \mathbb{R}^{T \times 32 \times 27}$ (Fig. 4.2) and $\mathbf{Y} \in \mathbb{R}^{T \times 3}$. The data were divided into training and test samples in the ratio of $\frac{1}{3}$.

We applied hankelization to the initial data with $\tau_0 = 10$ by temporal dimension and with $\tau_1 = 2$ by spatial dimension. So, the hankelized data along temporal dimension is $\underline{\mathbf{X}} \in \mathbb{R}^{(T-9)\times 10\times 32\times 27}$ and $\mathbf{Y} \in \mathbb{R}^{(T-9)\times 3}$, along space dimensions $\underline{\mathbf{X}} \in \mathbb{R}^{T\times 10\times 31\times 2\times 27}$ and $\mathbf{Y} \in \mathbb{R}^{T\times 3}$ and along both dimensions is $\underline{\mathbf{X}} \in \mathbb{R}^{(T-9)\times 10\times 31\times 2\times 27}$ and $\mathbf{Y} \in \mathbb{R}^{(T-9)\times 10\times 3}$.

Also, we used data from Neurotycho [17] dataset with 64 channels, to investigate how hankelization influence quality of prediction for more complex data.

4.1.2 Multimodal EEG dataset

The dataset includes 60-channel electroencephalography (EEG), see Fig. 4.5-4.6, and 7-channel electromyography (EMG), see Fig. 4.3-4.4. Subjects performed different upper-extremity movement tasks. The EEG data were filtered by authors between 8 and 30 Hz (μ and β bands, respectively), known to be within the motor-related frequency range. Besides, artifact rejection was performed. The original EEG signals are converted into a space time representation using a wavelet transform with a Morlet wavelet. The frequencies were chosen between 8 and 30 Hz with step equals 1 Hz. So, $\underline{\mathbf{X}} \in \mathbb{R}^{T\times 64\times 24}$, where 24 is a number of frequencies. $\mathbf{Y} \in \mathbb{R}^{T\times 6}$ is the EMG data.

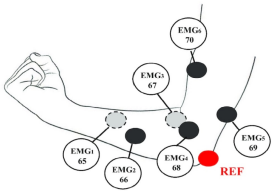

Figure 4.3: EMG electodes positions

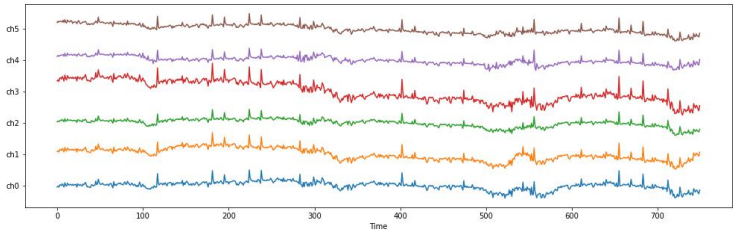

Figure 4.4: EMG data

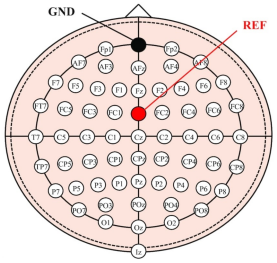

Figure 4.5: EMG electodes positions

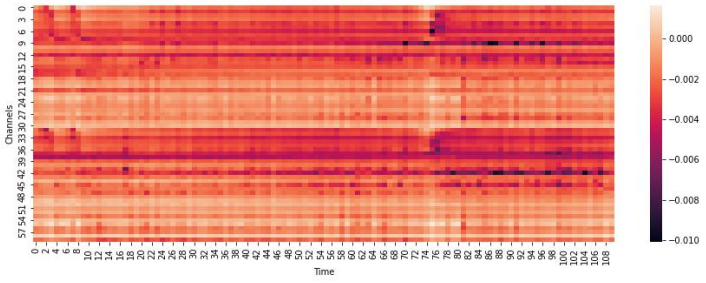

Figure 4.6: EEG data

4.2 Quality criteria

The scaled Root Mean Squared Error (sRMSE) shows the quality of the model prediction. We estimate sRMSE on train and test data.

$$\text{sRMSE}(\underline{\mathbf{Y}}, \widehat{\underline{\mathbf{Y}}}_{\mathbf{a}}) = \sqrt{\frac{\text{MSE}(\underline{\mathbf{Y}}, \widehat{\underline{\mathbf{Y}}}_{\mathbf{a}})}{\text{MSE}(\underline{\mathbf{Y}}, \overline{\underline{\mathbf{Y}}})}} = \frac{\|\underline{\mathbf{Y}} - \widehat{\underline{\mathbf{Y}}}_{\mathbf{a}}\|_2}{\|\underline{\mathbf{Y}} - \overline{\underline{\mathbf{Y}}}\|_2}. \tag{4.1}$$

Here $\widehat{\underline{\mathbf{Y}}}_{\mathbf{a}} = \underline{\mathbf{X}}_{\mathbf{a}}\underline{\boldsymbol{\Theta}}_{\mathbf{a}}^{\mathsf{T}}$ is a model prediction and $\overline{\underline{\mathbf{Y}}}$ is a constant prediction obtained by averaging the targets across all objects. The error on the test set should be as minimal as possible.

To evaluate the complexity of models, we looked at shape of the latent representations of the initial data. Also, for graph to compare models, the number of values in latent representation of $\underline{\mathbf{X}}$, N_{values} was used. For latent tensor $\hat{\underline{\mathbf{X}}} \in \mathbb{R}^{L_1 \times \ldots \times L_G}$, N_{values} is calculated as follows:

$$N_{values} = L_1 \cdot \ldots \cdot L_G.$$

4.3 Results

In this section the results for three models and three datasets are presented. We divided each sample on ten subsamples of five minutes length.

4.3.1 MPCA

We used MPCA as the most simple tensor dimensionality reduction model. We used MPCA that saves 97% of information. Shapes of latent variables for $\underline{\mathbf{X}}$ and $\underline{\mathbf{Y}}$ can be seen in the Table 4.1. Then, we trained Tucker tensor regression with ranks for each tensor mode as hyperparameters. Optimal hyperparameters were found by grid search. For this model, the optimal type of tensorization mostly is hankelization along space dimension. It can be seen on Figures 4.8-4.9. However, no tensorization gives fewer number of values in latent representation of $\underline{\mathbf{X}}$. It can be noticed in Fig. 4.7-4.9.

Table 4.1: Results with MPCA

Dataset	Hankelization	Shape of the latent variable of $\underline{\mathbf{X}}$	Shape of the latent variable of $\underline{\mathbf{Y}}$	sRMSE
Neurotycho A	No	1×8	3	$\mathbf{1.727 \pm 0.043}$
	Along spatial dim	$10 \times 1 \times 8$	8×3	1.737 ± 0.042
	Along temporal dim	$1 \times 7 \times 2$	3	1.878 ± 0.067
	Along both dims	$10 \times 1 \times 7 \times 2$	8×3	1.912 ± 0.072
Neurotycho K	No	1×27	3	4.241 ± 0.506
	Along spatial dim	$10 \times 1 \times 26$	4×3	4.067 ± 0.474
	Along temporal dim	$1 \times 22 \times 2$	3	4.173 ± 0.487
	Along both dims	$10 \times 1 \times 21 \times 2$	4×3	$\mathbf{4.038 \pm 0.439}$
EEG	No	1×10	3	1.766 ± 0.190
	Along spatial dim	$9 \times 1 \times 11$	9×4	$\mathbf{1.699 \pm 0.222}$
	Along temporal dim	$1 \times 14 \times 2$	3	2.499 ± 0.353
	Along both dims	$9 \times 1 \times 14 \times 2$	9×4	2.635 ± 0.498

4.3.2 HOPLS

HOPLS is more complex model than MPCA as it makes an alignment between features and targets. Fitting of the model tunes the number of latent tensors by maximizing the metric. We chose a metric connected with sRMSE 4.1 which equals $1 - sRMSE$. The hyperparameters of the HOPLS model are the shapes of latent representations of $\underline{\mathbf{X}}$ and $\underline{\mathbf{Y}}$. The optimal hyperparameters were found by grid search. The optimal shapes of core tensor of HOPLS are in Table 4.2. For two datasets, the optimal type of tensorization is hankelization along both dimensions. For the Human EEG dataset,

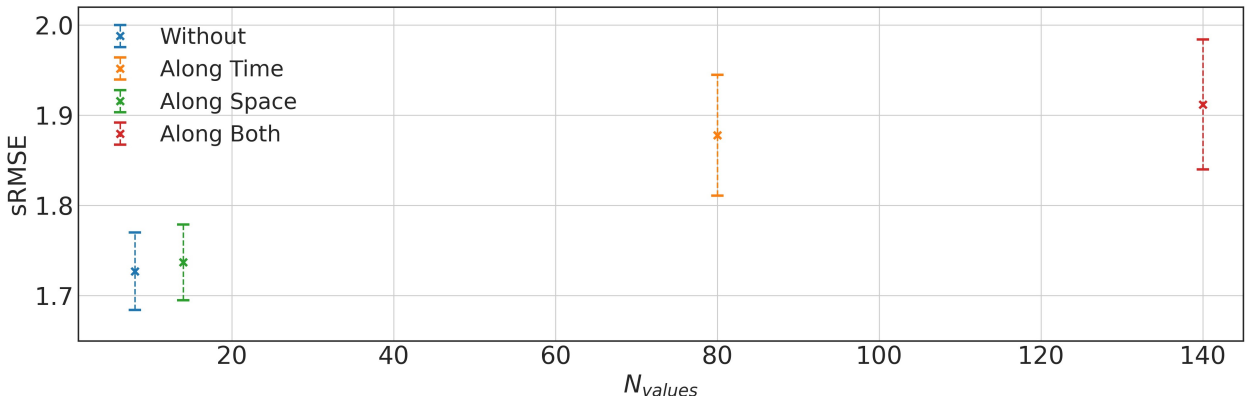

Figure 4.7: Comparison of models for Neurotycho dataset (ch=32) and MPCA model

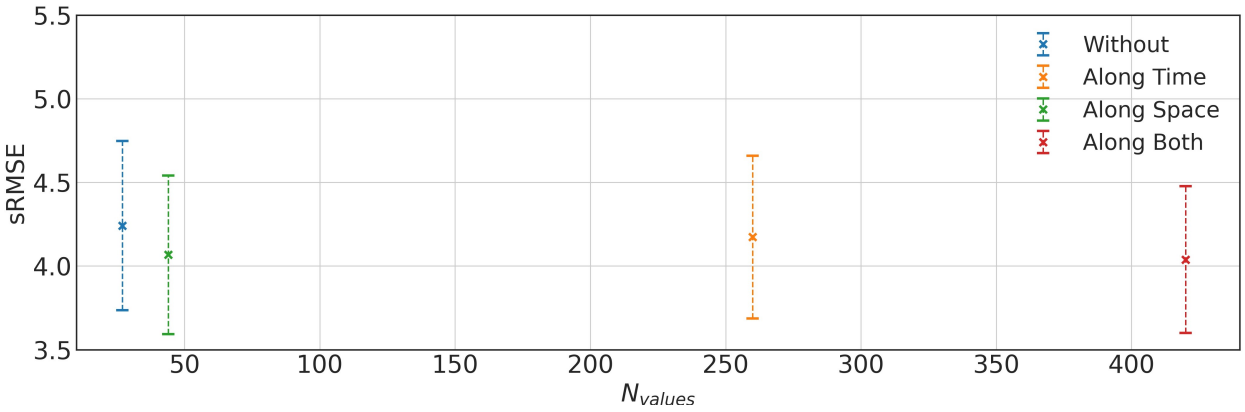

Figure 4.8: Comparison of models for Neurotycho dataset (ch=64) and MPCA model

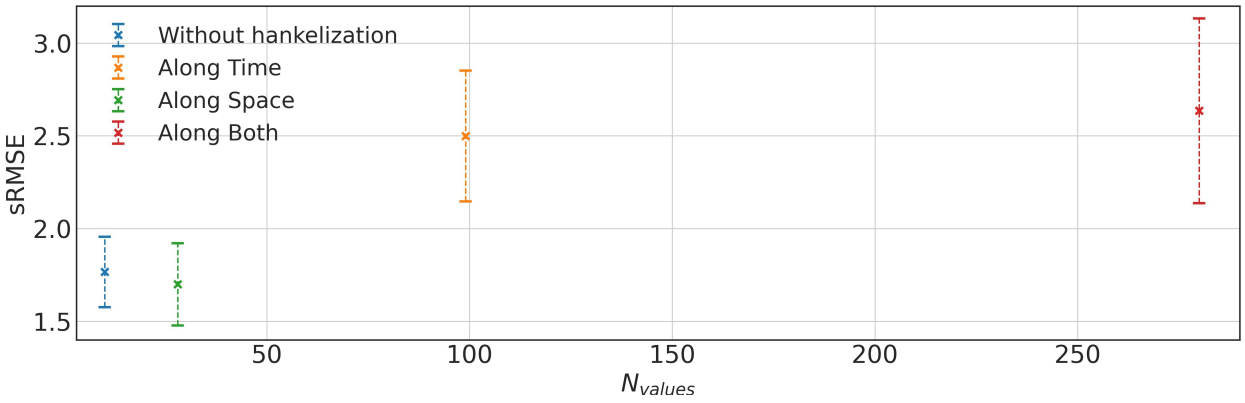

Figure 4.9: Comparison of models for Human EEG dataset (ch=60) and MPCA model

the smallest metric was observed without hankelization. However, the fewest number of the values of latent representations was obtained by hankelization along space dimension. It can be seen on Fig. 4.10-4.12.

4.3.3 TensorReducedNet

We decreased dimensionality only of $\underline{\mathbf{X}}$ by TensorReducedNet. So, to evaluate complexity of this deep learning model we additionally estimated the number of parameters of the neural network.

Table 4.2: Results with HOPLS

Dataset	Hankelization	Shape of the latent variable of $\underline{\mathbf{X}}$	Shape of the latent variable of $\underline{\mathbf{Y}}$	sRMSE
Neurotycho A	No	2×3	1	1.656 ± 0.050
	Along spatial dim	$\mathbf{3 \times 1 \times 1}$	1×1	1.444 ± 0.063
	Along temporal dim	$2 \times 2 \times 1$	1	$\mathbf{1.250 \pm 0.067}$
	Along both dim	$2 \times 3 \times 3 \times 1$	3×1	1.415 ± 0.054
Neurotycho K	No	1×1	1	3.316 ± 0.424
	Along spatial dim	$2 \times 3 \times 1$	1×1	3.688 ± 0.451
	Along temporal dim	$\mathbf{2 \times 1 \times 2}$	1	3.044 ± 0.528
	Along both dims	$1 \times 2 \times 2 \times 2$	1×2	$\mathbf{2.782 \pm 0.499}$
EEG	No	1×8	1	1.324 ± 0.131
	Along spatial dim	$2 \times 3 \times 7$	2×1	$\mathbf{1.322 \pm 0.133}$
	Along temporal dim	$\mathbf{3 \times 1 \times 2}$	1	1.805 ± 0.196
	Along both dims	$2 \times 2 \times 5 \times 2$	1×4	1.797 ± 0.216

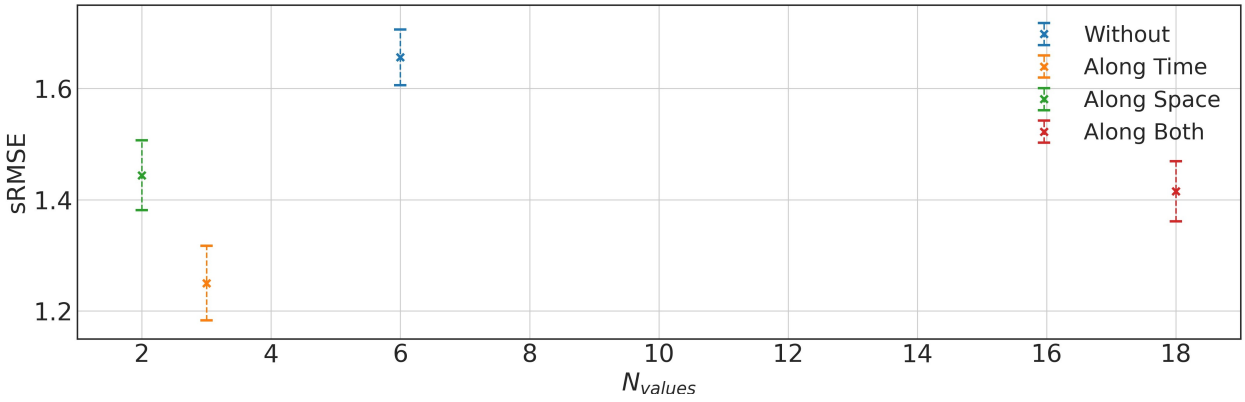

Figure 4.10: Comparison of models for Neurotycho dataset (ch=32) and HOPLS model

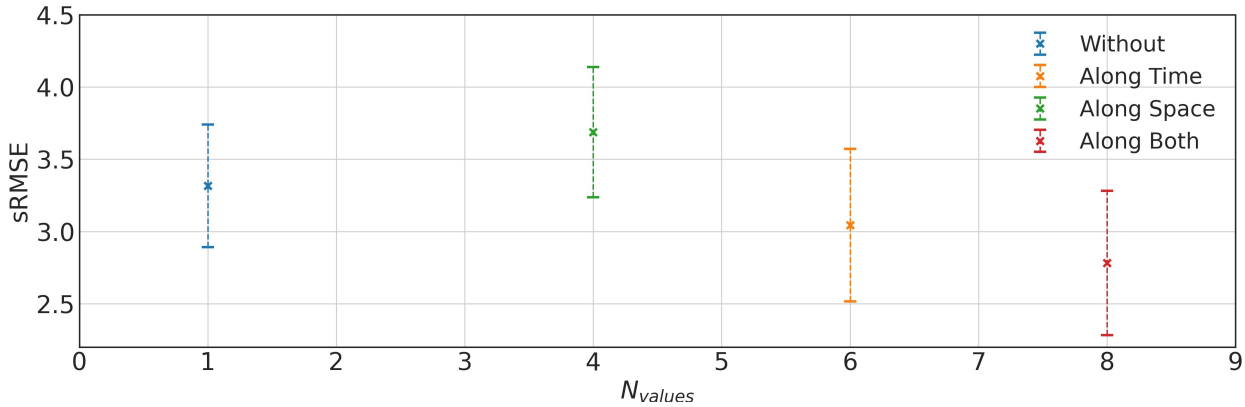

Figure 4.11: Comparison of models for Neurotycho dataset (ch=64) and HOPLS model

The hyperparameter of this model is the shape of the latent representation of $\underline{\mathbf{X}}$. It was tuned by grid search.

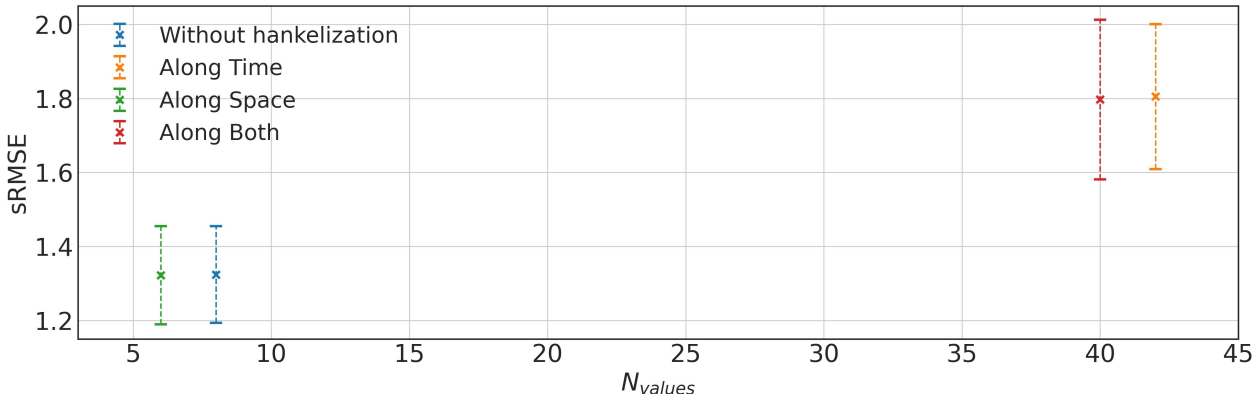

Figure 4.12: Comparison of models for Human EEG dataset (ch=60) and HOPLS model

Table 4.3: Results with TensorReducedNet with loss function $\mathcal{L}_1$ (3.5)

Dataset	Hankelization	Shape of the latent variable of $\underline{\mathbf{X}}$	sRMSE
Neurotycho A	No	7×6	1.032 ± 0.031
	Along spatial dimension	$5 \times 5 \times 1$	$\mathbf{1.015 \pm 0.024}$
	Along temporal dimension	$\mathbf{4 \times 3 \times 1}$	1.146 ± 0.050
	Along both dimensions	$3 \times 1 \times 3 \times 2$	1.120 ± 0.032
Neurotycho K	No	8×10	$\mathbf{0.956 \pm 0.041}$
	Along spatial dimension	$\mathbf{8 \times 2 \times 1}$	1.003 ± 0.048
	Along temporal dimension	$3 \times 3 \times 2$	1.167 ± 0.084
	Along both dimensions	$3 \times 3 \times 3 \times 1$	1.117 ± 0.141
EEG	No	12×8	1.352 ± 0.151
	Along spatial dimension	$\mathbf{4 \times 1 \times 1}$	$\mathbf{1.338 \pm 0.105}$
	Along temporal dimension	$4 \times 1 \times 3$	1.636 ± 0.210
	Along both dimensions	$3 \times 1 \times 4 \times 2$	1.476 ± 0.260

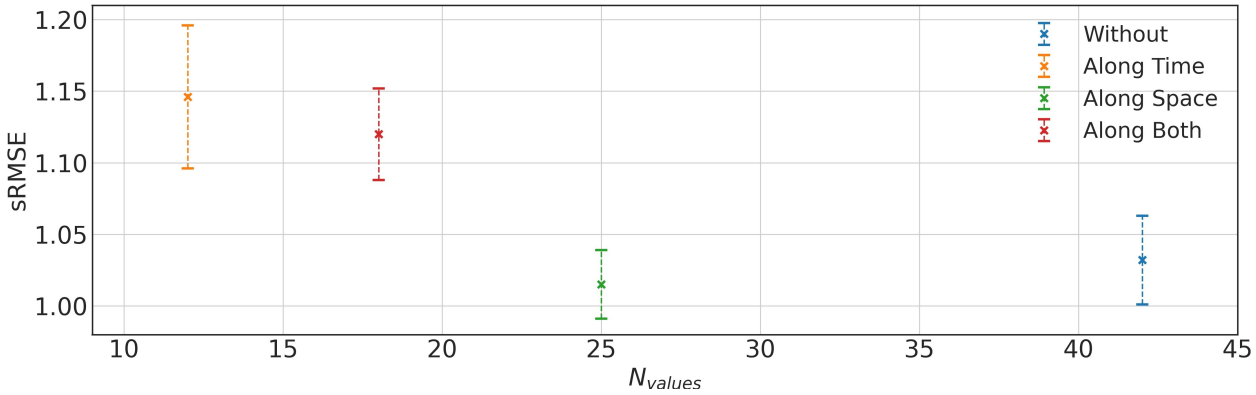

Figure 4.13: Comparison of models for Neurotycho dataset (ch=32) and AutoEncoder

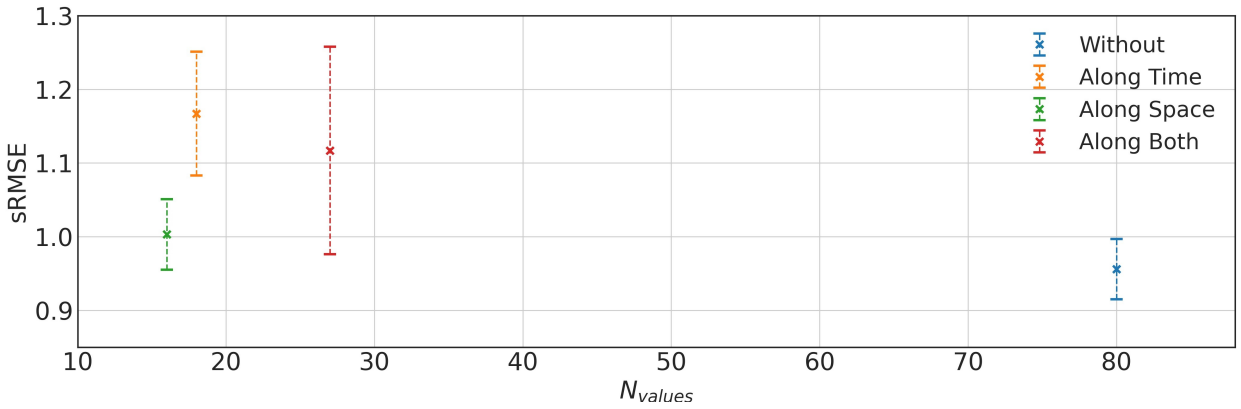

Figure 4.14: Comparison of models for Neurotycho dataset (ch=64) and AutoEncoder

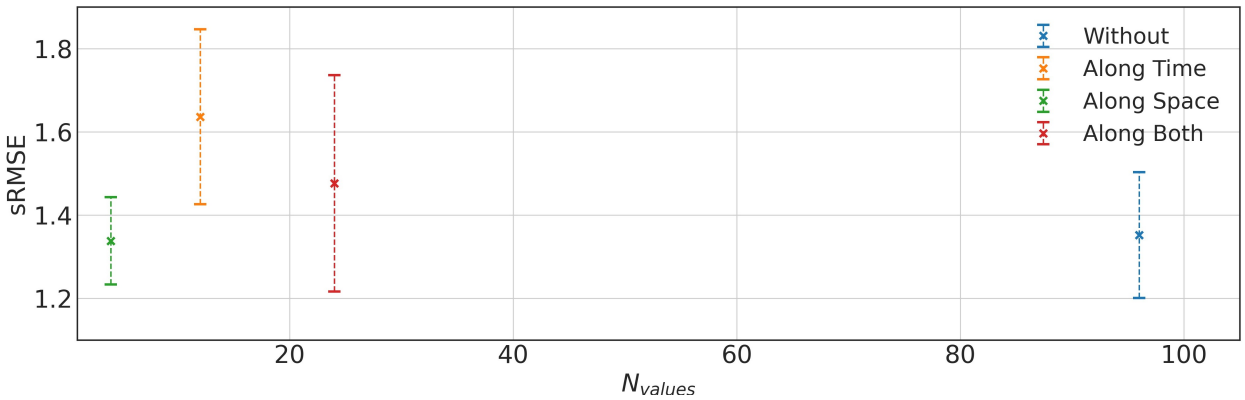

Figure 4.15: Comparison of models for Human EEG dataset (ch=60) and AutoEncoder

Chapter 5
Discussion and conclusion

In this work, the influence of hankelization on forecasting quality was studied. We tested hankelization on three datasets and before three dimensionality reduction models.

Previously it was shown [16] that the forecasting of time series for other then BCi task is better with hankelization only along temporal dimension. Our results showed that for BCI, hankelization along spatial dimension works the best way for MPCA in many cases. For HOPLS, hankelization along temporal and spatial dimensions works better than only along temporal dimension. It can be because of high correlation between data from different electrodes.

Bibliography

[1] Bengio, Y., and Lecun, Y. Convolutional networks for images, speech, and time-series.

[2] Chao, Z. C., Nagasaka, Y., and Fujii, N. Long-term asynchronous decoding of arm motion using electrocorticographic signals in monkeys. *Frontiers in Neuroengineering 3* (2010).

[3] Cichocki, A., Phan, A.-H., Zhao, Q., Lee, N., Oseledets, I., Sugiyama, M., Mandic, D. P., et al. Tensor networks for dimensionality reduction and large-scale optimization: Part 2 applications and future perspectives. *Foundations and Trends® in Machine Learning 9*, 6 (2017), 431–673.

[4] Eliseyev, A., and Aksenova, T. Penalized multi-way partial least squares for smooth trajectory decoding from electrocorticographic (ecog) recording. *PloS one* (2016), 11(5).

[5] Eyndhoven, S., Bousse, M., Hunyadi, B., Lathauwer, L., and Huffel, S. *Single-channel EEG classification by multi-channel tensor subspacelearning and regression*. IEEE interentional workshop on machine learning for signel processing, 2018.

[6] Jeong, J. H., Cho, J. H., Shim, K. H., Kwon, B. H., Lee, B. H., Lee, D. Y., Lee, D. H., and Lee, S. W. Multimodal signal dataset for 11 intuitive movement tasks from single upper extremity during multiple recording sessions. *GigaScience 9* (2020).

[7] Ji, T., Jiang, Y., Li, M., and Wu, Q. Ultra-short-term wind speed and wind power forecast via selective hankelization and low-rank tensor learning-based predictor. *International Journal of Electrical Power and Energy Systems 140* (2022).

[8] Lemm, S., Blankertz, B., Curio, G., and Müller, K. R. Spatio-spectral filters for improving the classification of single trial eeg. *IEEE Transactions on Biomedical Engineering 52* (2005).

[9] Li, Y., Yang, M., and Zhang, Z. A survey of multi-view representation learning. *IEEE Transactions on Knowledge and Data Engineering 31* (2019).

[10] Lu, H., Plataniotis, K. N., and Venetsanopoulos, A. N. Mpca: Multilinear principal component analysis of tensor objects. *IEEE transactions on Neural Networks 19*, 1 (2008), 18–39.

[11] Miller, K. J. A library of human electrocorticographic data and analyses. *Nature human behaviour 3*, 11 (2019), 1225–1235.

[12] Motrenko, A., and Strijov, V. Multi-way feature selection for ecog-based brain-computer interface. *Expert Systems with Applications 114* (2018), 402–413.

[13] Onishi, A., Phan, A. H., Matsuoka, K., and Cichocki, A. Tensor classification for p300-based brain computer interface.

[14] Ran, X., Chen, W., Yvert, B., and Zhang, S. A hybrid autoencoder framework of dimensionality reduction for brain-computer interface decoding. *Computers in Biology and Medicine* (2022), 148.

[15] Shen, Z., Liu, B., Zhou, Q., Liu, Z., Xia, B., and Li, Y. Cost-sensitive tensor-based dual-stage attention lstm with feature selection for data center server power forecasting. *ACM Transactions on Intelligent Systems and Technology* (10 2022).

[16] Shi, Q., Yin, J., Cai, J., Cichocki, A., Yokota, T., Chen, L., Yuan, M., and Zeng, J. Block hankel tensor arima for multiple short time series forecasting.

[17] Shimoda, K., Nagasaka, Y., Chao, Z. C., and Fujii, N. Decoding continuous three-dimensional hand trajectories from epidural electrocorticographic signals in japanese macaques. *Journal of neural engineering* (2012), 9(3).

[18] Wang, X., Miranda-Moreno, L., and Sun, L. Hankel-structured tensor robust pca for multi-variate traffic time series anomaly detection.

[19] Wong, H. S., Wang, L., Chan, R., and Zeng, T. Deep tensor cca for multi-view learning. *IEEE Transactions on Big Data 8* (2022).

[20] Yokota, T., Erem, B., Guler, S., Warfield, S. K., and Hontani, H. Missing slice recovery for tensors using a low-rank model in embedded space.

[21] Zhao, Q., Caiafa, C. F., Mandic, D. P., Chao, Z. C., Nagasaka, Y., Fujii, N., Zhang, L., and Cichocki, A. Higher order partial least squares (hopls): A generalized multilinear regression method. *IEEE Transactions on Pattern Analysis and Machine Intelligence 35* (2013).

[22] Zhao, Q., Zhang, L., and Cichocki, A. Multilinear and nonlinear generalizations of partial least squares: an overview of recent advances. *Wiley Interdiscip. Rev. Data Min. Knowl. Discov. 4*, 2 (2014), 104–115.

[23] Zhou, G., Zhao, Q., Zhang, Y., Adali, T., Xie, S., and Cichocki, A. Linked component analysis from matrices to high-order tensors: Applications to biomedical data. *Proceedings of the IEEE 104* (2 2016), 310–331.